KBB-Forum
2026;25(3)
www.KBB-Forum.net

CLINICAL STUDY

COMPUTED TOMOGRAPHY AND NON-EPI DWI IN PEDIATRIC CHOLESTEATOMA: COMPLEMENTARY ROLES IN PREOPERATIVE AND POSTOPERATIVE EVALUATION

Seda Kaynak ŞAHAP [1], MD, Eda ALMUS [1], MD, Emre OCAK [2], MD, Selçuk MÜLAZIMOĞLU [2], MD, Ömer Göktuğ TÜFEKÇİ [2], MD, Seher YÜKSEL [3], MD, Suat FİTOZ [1], MD

[1]*Ankara Üniversitesi Tıp Fakültesi, Çocuk Radyolojisi Bilim Dalı, Ankara, Türkiye*
[2]*Ankara Üniversitesi Tıp Fakültesi, Kulak Burun ve Boğaz Hastalıkları Anabilim Dalı, Ankara, Türkiye*
[3]*Ankara Üniversitesi Tıp Fakültesi, Patoloji Anabilim Dalı, Ankara, Türkiye*

ABSTRACT

Purpose

To evaluate computed tomography (CT) and magnetic resonance imaging (MRI) findings in surgically and histopathologically confirmed pediatric cholesteatoma and to investigate the correlation between CT-visible soft tissue and diffusion restriction on non-echo-planar diffusion-weighted imaging (non-EPI DWI) in preoperative and postoperative settings.

Materials and Methods

This retrospective descriptive study included 16 pediatric patients (20 ears) with surgically and histopathologically confirmed cholesteatoma who underwent temporal bone CT and/or MRI. CT findings, including lesion location and osseous abnormalities, were evaluated, and ossicular erosion was correlated with operative findings where available. CT–DWI correlation was classified as complete, partial, or discordant according to the extent of diffusion restriction relative to CT-visible soft tissue. Continuous variables were summarized as mean ± standard deviation (SD), whereas categorical variables were presented as frequencies and percentages.

Results

Preoperative CT demonstrated mastoid opacification in 85.7% of ears and osseous erosive changes in 71.4%. CT showed complete agreement with surgery for malleus erosion, whereas stapes evaluation was frequently limited by surrounding soft tissue. Diffusion restriction was identified in 21 of 22 MRI examinations (95.5%). Mastoid opacification rarely demonstrated corresponding diffusion restriction. Complete CT–DWI correlation was observed in nine examinations and partial correlation in six, occurring more frequently in postoperative studies.

Conclusion

CT provides valuable anatomical information and accurately depicts osseous involvement, whereas non-EPI DWI more accurately reflects the true extent of cholesteatoma. The discrepancy between CT-visible soft tissue and diffusion restriction was more apparent in the postoperative setting, where CT may overestimate the extent of recurrent disease.

Keywords: *Pediatric cholesteatoma; Computed tomography; Non-echo-planar diffusion-weighted imaging; Magnetic resonance imaging; Temporal bone*

Pediatrik Kolesteatomda Bilgisayarlı Tomografi ve Non-EPI Difüzyon Ağırlıklı MR Görüntülemenin Preoperatif ve Postoperatif Değerlendirmedeki Tamamlayıcı Rolleri

ÖZET

Amaç

Bu çalışmanın amacı, cerrahi ve histopatolojik olarak doğrulanmış pediatrik kolesteatom olgularında bilgisayarlı to-

mografi (BT) ve manyetik rezonans görüntüleme (MRG) bulgularını değerlendirmek ve hem preoperatif hem de postoperatif dönemde BT'de izlenen yumuşak doku ile non-eko-planar difüzyon ağırlıklı görüntülemede (non-EPI DWI) saptanan difüzyon kısıtlanması arasındaki ilişkiyi incelemektir.

Gereç ve Yöntem

Bu retrospektif tanımlayıcı çalışmaya, temporal kemik BT ve/veya MRG incelemesi bulunan, cerrahi ve histopatolojik olarak doğrulanmış kolesteatom tanılı 16 pediatrik hasta (20 kulak) dahil edildi. BT'de lezyon lokalizasyonu ve kemik değişiklikleri değerlendirildi; kemikçik erozyonları uygun olgularda cerrahi bulgular ile karşılaştırıldı. BT–DWI uyumu, difüzyon kısıtlanmasının BT'de görülen yumuşak dokuya göre yaygınlığı esas alınarak tam, parsiyel veya uyumsuz olarak sınıflandırıldı. Sürekli değişkenler ortalama ± standart sapma (SS), kategorik değişkenler ise sayı ve yüzde olarak sunuldu.

Bulgular

Preoperatif BT'de değerlendirilen kulakların %85,7'sinde mastoid opasifikasyon, %71,4'ünde kemik destrüksiyonu saptandı. Malleus erozyonunda BT ile cerrahi bulgular arasında tam uyum izlenirken, stapes değerlendirmesi çevresindeki yumuşak dokular nedeniyle sıklıkla sınırlı kaldı. Difüzyon kısıtlanması 22 MRG incelemesinin 21'inde (%95,5) saptandı. Mastoid opasifikasyonuna karşılık gelen difüzyon kısıtlanması nadiren izlendi. Dokuz incelemede tam BT–DWI uyumu, altı incelemede ise parsiyel uyum saptandı; parsiyel uyum postoperatif incelemelerde daha sık görüldü.

Sonuç

BT anatomik değerlendirmede önemli bilgiler sağlamakta ve kemik tutulumunu doğru bir şekilde göstermekteyken, non-EPI DWI kolesteatomun gerçek yaygınlığını daha doğru yansıtmaktadır. BT'de izlenen yumuşak doku ile difüzyon kısıtlanması arasındaki uyumsuzluk postoperatif dönemde daha belirgin olup, BT rekürren hastalığın yaygınlığını olduğundan fazla gösterebilir.

Anahtar kelimeler: *Pediatrik kolesteatom; Bilgisayarlı tomografi; Non-eko-planar difüzyon ağırlıklı görüntüleme; Manyetik rezonans görüntüleme; Temporal kemik*

INTRODUCTION

Cholesteatoma is a locally destructive lesion characterized by the accumulation of keratinizing squamous epithelium within the middle ear and mastoid cavity. Although histologically benign, it may cause progressive bone erosion and lead to serious complications, including hearing loss, facial nerve palsy, labyrinthine fistula, and intracranial infection if left untreated[1–3]. Compared with adults, pediatric cholesteatoma generally demonstrates more aggressive behavior, with more extensive disease at presentation and a higher risk of residual or recurrent disease after surgery[4,5].

Imaging plays a central role in the diagnosis and management of pediatric cholesteatoma. High-resolution computed tomography (CT) is the primary imaging modality for evaluating disease extent and associated osseous changes, including scutum blunting, ossicular erosion, facial canal dehiscence, and tegmen defects[2,6]. However, CT has limited specificity because soft-tissue opacification may represent cholesteatoma as well as granulation tissue, postoperative fibrosis, inflammatory tissue, or middle ear effusion[2,7]. This limitation is particularly important in the postoperative setting, where recurrent cholesteatoma must be distinguished from expected postoperative changes[2,3].

Non-echo-planar diffusion-weighted magnetic resonance imaging (non-EPI DWI) has substantially improved the radiologic evaluation of cholesteatoma

Corresponding Author: Seda KAYNAK ŞAHAP, Ankara Üniversitesi Tıp Fakültesi, Çocuk Radyolojisi Bilim Dalı, Ankara, Türkiye
E-Posta:dr.seda@gmail.com,
Received: 02 July 2026 , **Revised for: 25 August 2026**, **Accepted for publication: 15 September2026**
Cite this article: ŞAHAP S., ALMUS E., OCAK E., MÜLAZIMOĞLU S., TÜFEKÇİ Ö.G., YÜKSEL S., FİTOZ S. Computed Tomography and Non-EPI DWI in Pediatric Cholesteatoma: Complementary Roles in Preoperative and Postoperative Evaluation KBB-Forum 2026; 25 (3) 145 - 155

because of its high diagnostic accuracy for detecting keratin-containing lesions[8,9]. Consequently, it has become the preferred imaging technique for identifying residual or recurrent cholesteatoma and has significantly reduced the need for routine second-look surgery in many centers[3,8]. Although the complementary roles of CT and non-EPI DWI in cholesteatoma are well established, direct comparison of disease extent on CT and DWI in surgically confirmed pediatric cases remains limited, particularly in preoperative and postoperative settings. Such comparison may help distinguish cholesteatoma from inflammatory or postoperative changes.

Therefore, the aim of this study was to evaluate CT and MRI findings in surgically and histopathologically confirmed pediatric cholesteatoma and, more specifically, to investigate the spatial relationship between CT-visible soft-tissue opacification and diffusion restriction on non-EPI DWI in the preoperative and postoperative settings.

MATERIALS and METHODS

Study Design and Patients

This retrospective descriptive study was conducted at a tertiary referral center after obtaining approval from the institutional ethics committee. The requirement for informed consent was waived because of the retrospective nature of the study.

Pediatric patients with surgically treated primary or recurrent cholesteatoma who underwent preoperative and/or postoperative temporal bone CT and MRI examinations between March 2014 and May 2026 were identified from the institutional radiology and surgical databases.

Patients with histopathologically confirmed cholesteatoma and available imaging studies were included. Patients with inadequate image quality, incomplete imaging data, or lacking histopathological confirmation of cholesteatoma were excluded. A total of 16 pediatric patients were included in the study. Because four patients had bilateral disease, imaging findings were analyzed by ear, resulting in a total of 20 ears.

Image Protocol

Temporal bone CT examinations were performed using a 64-detector CT scanner (Ingenuity, Philips Medical Systems, Eindhoven, The Netherlands). Images were acquired at 120 kVp and 200 mAs and reconstructed with 0.67-mm isotropic reconstructions using a high-resolution bone algorithm.

MRI examinations were performed on a 1.5-T scanner (Ingenia, Philips Medical Systems, Eindhoven, The Netherlands). The imaging protocol included axial and coronal T1-weighted images (TR/TE, 550/10 ms; slice thickness, 3 mm; FOV, 150 mm), T2-weighted images (TR/TE, 3000/120 ms; slice thickness, 3 mm; FOV, 150 mm), and turbo spin-echo diffusion-weighted imaging (TSE-DWI) sequence using a non-echo-planar (non-EPI) technique (TR/TE, 2833/75 ms; slice thickness, 3 mm; FOV, 180 × 150 mm; matrix, 100 × 72). Post-contrast T1-weighted images were obtained when clinically indicated.

Radiological Evaluation

Temporal bone CT and MRI examinations were reviewed retrospectively by a pediatric radiologist with 10 years of experience.

For preoperative CT examinations, the following findings were recorded: lesion location (Prussak space, epitympanum, mesotympanum, hypotympanum, aditus ad antrum, antrum, mastoid cavity, and external auditory canal), the presence of mastoid opacification, scutum blunting, ossicular erosion, tegmen tympani erosion, facial canal dehiscence/erosion, lateral semicircular canal fistula, and the presence of other osseous erosive changes. Ossicular erosion was evaluated separately for the malleus, incus, and stapes. When ossicular integrity could not be reliably determined because of surrounding soft tissue, the finding was recorded as indeterminate. Surgical reports were reviewed for correlation where available. If the operative findings did not explicitly describe the integrity of an individual ossicle, the surgical status was classified as not assessable rather than assumed to be intact or eroded.

For preoperative MRI examinations, the following MRI findings were evaluated: T1- and T2-weighted signal characteristics, the presence of diffusion restriction within the middle ear cavity and mastoid, and apparent diffusion coefficient (ADC) values. For postoperative MRI examinations, recurrent choleste-

atoma was diagnosed based on diffusion restriction and subsequently confirmed by surgery and histopathology.

For ears with both CT and MRI examinations available, either preoperatively or postoperatively, the correlation between CT-visible soft-tissue opacity and diffusion restriction on MRI was assessed. Complete correlation was defined as diffusion restriction involving the entire CT-visible soft-tissue opacity. Partial correlation was defined as diffusion restriction involving only part of the CT-visible soft tissue, indicating that the extent of cholesteatoma was smaller than the overall CT-visible lesion. Discordance was defined as CT-visible soft tissue without corresponding diffusion restriction.

Statistical Analysis

Statistical analyses were performed using IBM SPSS Statistics version 23 (IBM Corp., Armonk, NY, USA). Continuous variables were expressed as mean ± standard deviation (SD) and range. Categorical variables were presented as frequencies and percentages. Differences in CT–DWI correlation patterns between preoperative and postoperative examinations were evaluated using Fisher's exact test. A two-sided p value <0.05 was considered statistically significant. Given the descriptive nature of the study and the limited sample size, no additional inferential or multivariable analyses were performed.

RESULTS

The study included 16 pediatric patients with a mean age of 11.76 ± 3.24 years (range, 7.6–16.8 years). Seven patients (43.8%) were female and nine (56.3%) were male. Disease was right-sided in five patients (31.3%), left-sided in seven (43.8%), and bilateral in four (25.0%), resulting in a total of 20 affected ears. Eleven patients (68.8%) had primary disease and five (31.3%) had recurrent disease.

Preoperative CT examinations were available for 14 ears. The Prussak space was the most frequently involved site, followed by the epitympanum and aditus ad antrum. Mastoid opacification was the most common additional CT finding and was observed in 12 ears (85.7%). Overall, osseous erosive changes were identified in 10 ears (71.4%). Scutum blunting and ossicular erosion were each identified in 8 ears (57.1%). No lateral semicircular canal fistula was identified. One patient presented with seizures, and imaging findings were consistent with meningitis secondary to complicated infected cholesteatoma (Figure 1). Detailed preoperative CT findings are summarized in Table 1.

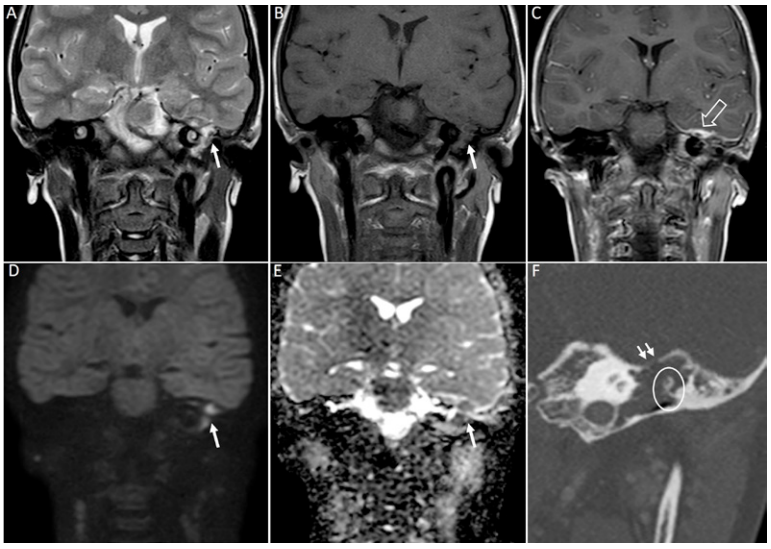

Figure 1. Contrast-enhanced temporal MRI (A–E) demonstrates a soft-tissue lesion occupying the epitympanum and mesotympanum (long white arrows), showing T2 hyperintensity (A), T1 isointensity (B), and diffusion restriction (D,E). Associated left temporobasal pachymeningeal enhancement (open arrow) is also present (C). Coronal non-contrast temporal bone CT (F) demonstrates a tegmen tympani defect (short arrows) and ossicular erosion (circle). The combined CT and MRI findings were highly suggestive of complicated infected cholesteatoma, subsequently confirmed at surgery and by histopathological examination.

Table 1. Preoperative CT Findings of Pediatric Cholesteatoma (n=14)

Finding	n (%)
Lesion location	
Prussak space involvement	13 (92.9)
Epitympanic involvement	12 (85.7)
Aditus ad antrum involvement	12 (85.7)
Mesotympanic involvement	11 (78.6)
Antral involvement	10 (71.4)
Hypotympanic involvement	6 (42.9)
External auditory canal involvement	5 (35.7)
Additional CT findings	
Mastoid opacification	12 (85.7)
Scutum blunting	8 (57.1)
Ossicular erosion	8 (57.1)
Tegmen tympani erosion	3 (21.4)
Facial canal dehiscence/erosion	3 (21.4)
Koerner septum defect	2 (14.3)

Correlation between CT and operative findings for ossicular erosion was evaluated only in ears with explicitly documented intraoperative ossicular status. For the malleus, CT findings were in complete agreement with surgery in all 13 assessable ears (6 erosions and 7 intact ossicles). For the incus, CT correctly identified erosion in 6 of 8 assessable surgically confirmed cases and correctly excluded erosion in both surgically intact ossicles, yielding an overall agreement of 8/10 (80.0%). Evaluation of the stapes was indeterminate on CT in 9 ears because it could not be reliably distinguished from the surrounding soft tissue. Among these 9 ears, stapes erosion was identified surgically in 8 (88.9%), suggesting that indeterminate CT assessment was frequently associated with stapes erosion.

A total of 22 MRI examinations were evaluated, including 12 preoperative and 10 postoperative studies; 16 had paired CT studies (10 preoperative and 6 postoperative). The remaining six unpaired MRI examinations comprised two preoperative and four postoperative studies. The median interval between surgery and postoperative MRI was 23.6 months (IQR, 14.8–30.9 months; range, 12.3–94.6 months).

Diffusion restriction was observed in 21 examinations (95.5%). Despite being one of the most frequent CT findings, mastoid opacification rarely demonstrated corresponding diffusion restriction on MRI (Figure 2). In most cases, the opacified mastoid cavity showed fluid signal intensity without diffusion restriction.

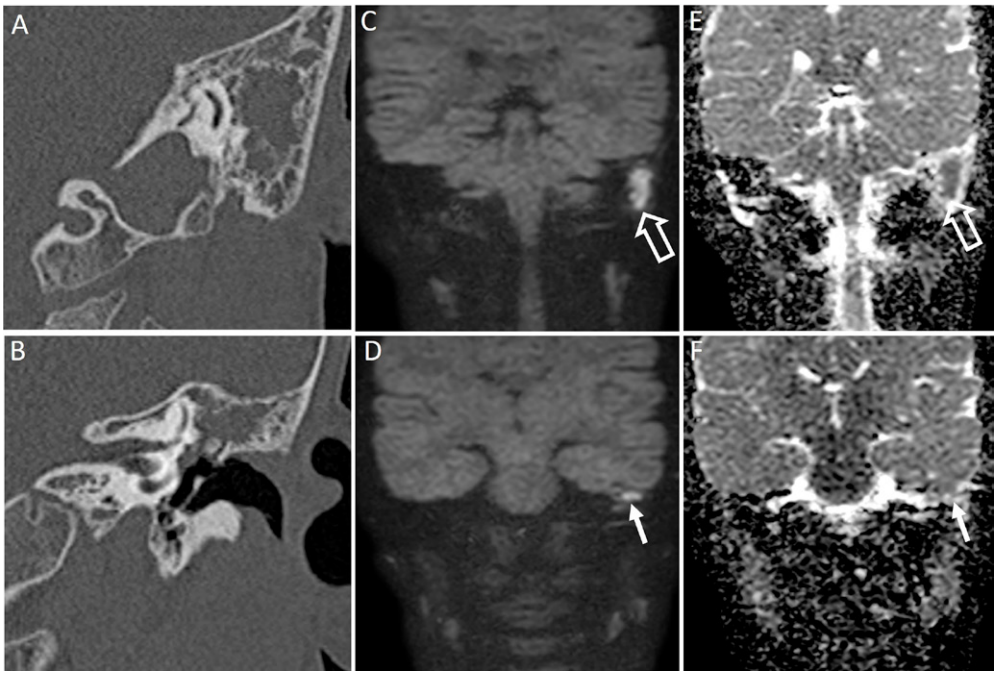

Figure 2. Non-contrast CT images (A, B) demonstrate extensive soft-tissue opacification involving the epitympanum, mesotympanum, and mastoid air cells. Corresponding non-EPI DWI MR images (C–F) demonstrate partial CT–DWI correlation (solid arrows) with additional diffusion restriction extending into the mastoid cavity (open arrows). Mastoid extension of the cholesteatoma was subsequently confirmed at surgery.

On T1-weighted images, lesions were most commonly isointense, whereas homogeneous T2 hyperintensity was the predominant signal characteristic. A small number of lesions demonstrated atypical T1 signal characteristics despite showing diffusion restriction and being confirmed as cholesteatoma at surgery. One of these lesions demonstrated interval enlargement on follow-up MRI before surgical confirmation (Figure 3).

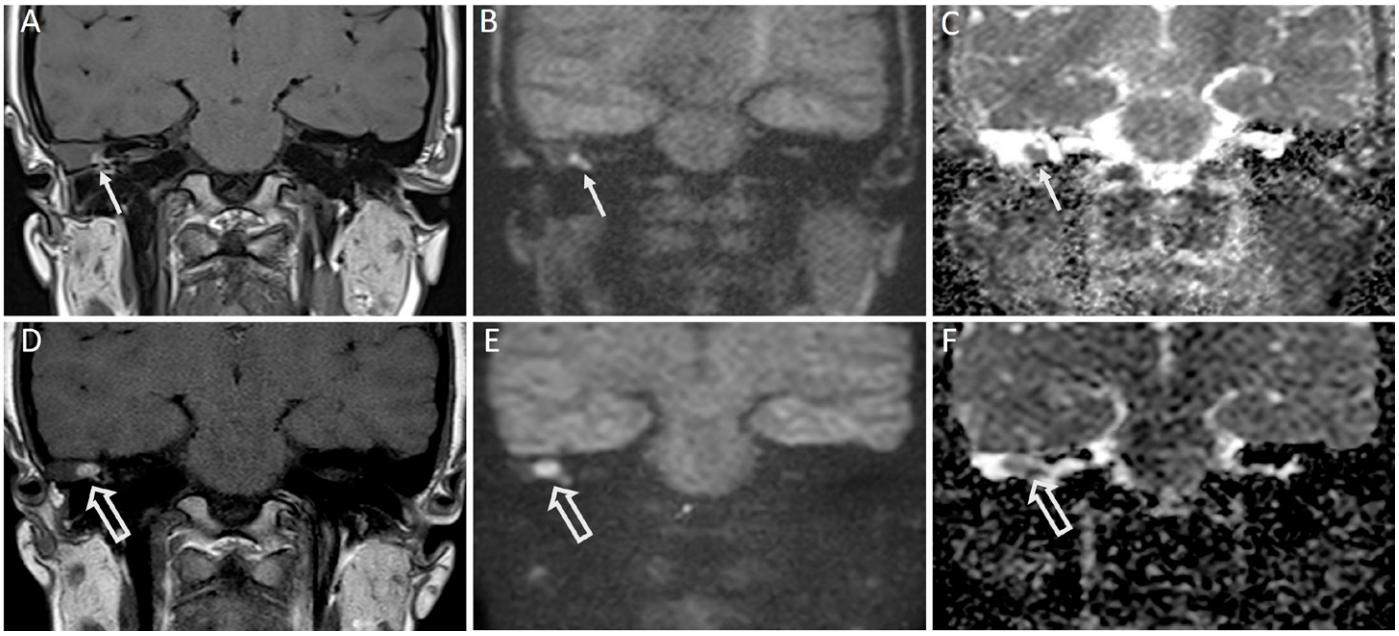

Figure 3. Initial postoperative MR images (A–C) demonstrate a T1-hyperintense lesion within the tympanomastoidectomy cavity showing diffusion restriction (solid arrows). Follow-up MR images obtained one year later (D–F) demonstrate interval enlargement of the lesion (open arrows). Although the T1 hyperintensity was considered atypical for cholesteatoma on imaging, surgery and histopathological examination confirmed recurrent cholesteatoma.

Postoperative lesions tended to demonstrate more heterogeneous signal characteristics than preoperative lesions. The mean ADC value of diffusion-restricting lesions was 879.5 ± 258.1 $\times 10^{-6}$ mm²/s (range, 408–1387 $\times 10^{-6}$ mm²/s). Detailed MRI findings are presented in Table 2.

Table 2. MRI Findings of Pediatric Cholesteatoma (n=22)

Finding	n (%)
Diffusion restriction	21 (95.5)
T1-weighted signal intensity	n (%)
Isointense	13 (59.1)
Hypointense	6 (27.3)
Heterogeneous/intermediate	2 (9.1)
Hyperintense	1 (4.5)
T2-weighted signal intensity	n (%)
Hyperintense	17 (77.3)
Heterogeneous/intermediate	4 (18.2)
Hypointense	1 (4.5)
ADC values	
Mean ± SD ($\times 10^{-6}$ mm²/s)	879.5 ± 258.1
Range ($\times 10^{-6}$ mm²/s)	408–1387

CT–DWI correlation was assessed in ears with both CT and MRI examinations available. Complete correlation was observed in 9 examinations, whereas partial correlation was observed in 6 examinations. Discordance, defined as CT-visible soft tissue without corresponding diffusion restriction, was observed in a single preoperative examination (Table 3).

Table 3. Correlation Between CT-Visible Soft Tissue and Diffusion Restriction on Non-EPI DWI

Correlation pattern	Preoperative	Postoperative	Total
Complete correlation	7	2	9
Partial correlation	2	4	6
Discordance	1	0	1

Complete CT–DWI correlation was more frequent in preoperative examinations than in postoperative ones (70% vs. 33%), whereas partial correlation was more common postoperatively (Figure 4). However, the difference was not statistically significant (Fisher's exact test, p = 0.302).

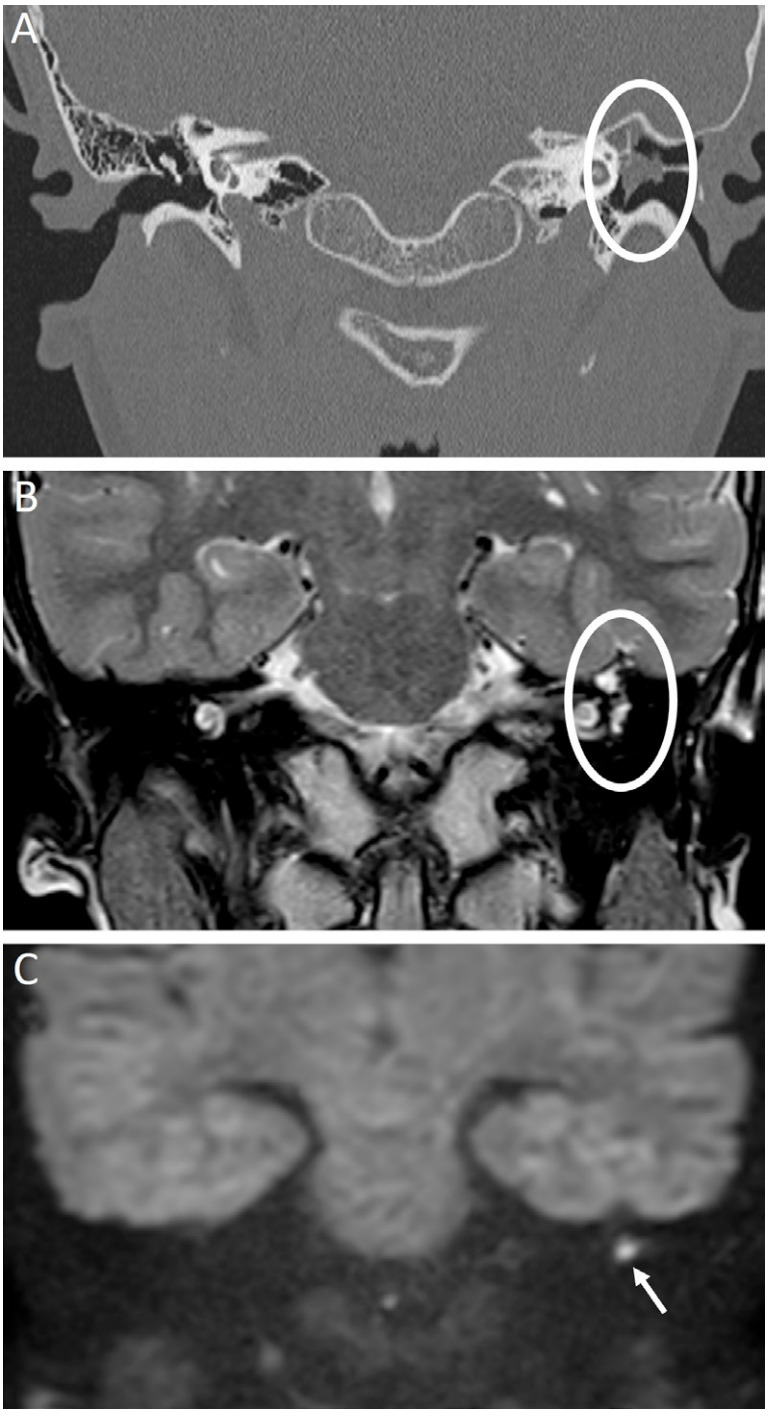

Figure 4. Postoperative non-contrast CT image (A) demonstrates soft tissue within the tympanomastoidectomy cavity (circle). Corresponding coronal T2-WI (B) and non-EPI DWI MR images (C) demonstrate partial CT–DWI correlation, with diffusion restriction compatible with recurrent cholesteatoma involving only part of the CT-visible soft tissue (arrow). Recurrent cholesteatoma was subsequently confirmed by surgery and histopathological examination.

DISCUSSION

The present study evaluated the CT and MRI characteristics of surgically and histopathologically confirmed pediatric cholesteatoma and investigated the relationship between CT-visible soft-tissue opacification and diffusion restriction on MRI in both preoperative and postoperative examinations. The main findings of our study were as follows: (1) the Prussak space was the most common site of disease involvement; (2) mastoid opacification was one of the most frequent CT findings but rarely demonstrated corresponding diffusion restriction on MRI; (3) CT accurately depicted most osseous abnormalities, although stapes evaluation was frequently limited by surrounding soft tissue; and (4) CT–DWI correlation tended to be more complete in preoperative than postoperative examinations, whereas postoperative lesions demonstrated more heterogeneous conventional MRI signal characteristics. An important contribution of our study is the direct comparison of CT-visible soft tissue with diffusion-restricting cholesteatoma, showing that their extent does not always correspond, particularly in the postoperative setting.

Pediatric cholesteatoma is generally considered more aggressive than adult disease because of its greater tendency for bone destruction, extensive disease, and recurrence1,5,6,10. Accurate imaging is therefore essential for both surgical planning and postoperative follow-up. High-resolution CT remains the imaging modality of choice for evaluating disease extent and osseous involvement owing to its excellent spatial resolution8. In our series, the Prussak space was the most frequently involved site, followed by the epitympanum and aditus ad antrum, consistent with the typical growth pattern of acquired pars flaccida cholesteatoma described

in previous studies[6]. Scutum blunting and ossicular erosion were also among the most common osseous abnormalities, reflecting the characteristic pattern of bone destruction in cholesteatoma. CT showed good agreement with operative findings for ossicular erosion, particularly for the malleus and incus, whereas reliable evaluation of the stapes remained challenging because it was frequently obscured by surrounding soft tissue. In our series, inability to confidently visualize the stapes on CT was frequently associated with underlying stapes erosion. These findings are consistent with previous reports demonstrating high CT accuracy for larger ossicles but lower diagnostic performance for the stapes because of its small size and complex anatomy[6,11]. However, previous CT studies have shown that chronic otitis media itself may also result in varying degrees of bone destruction, indicating that osseous erosion alone is insufficient for diagnosing cholesteatoma[12]. Moreover, soft-tissue opacification on CT lacks specificity because cholesteatoma, granulation tissue, fibrosis, and inflammatory tissue may demonstrate similar attenuation[1,6,8]. These limitations further emphasize the complementary role of MRI, particularly diffusion-weighted imaging, for accurate tissue characterization[8].

One of the most notable findings of our study was the discrepancy between mastoid opacification on CT and diffusion restriction on MRI. Although mastoid opacification was one of the most frequent CT findings, corresponding diffusion restriction within the mastoid cavity was identified only rarely. Furthermore, when diffusion restriction was present, it was confined to only a limited portion of the CT-visible mastoid soft tissue. Because chronic middle ear and mastoid inflammation is closely associated with pediatric acquired cholesteatoma, mastoid opacification on CT may frequently represent accompanying inflammatory changes rather than true cholesteatoma extension10. At the same time, mastoid extension is not uncommon in pediatric cholesteatoma and may complicate surgical management[6]. Therefore, mastoid opacification on CT should be interpreted cautiously and assessed together with diffusion-weighted MRI to avoid both overestimating and underestimating true cholesteatoma extension.

The complementary role of MRI became even more evident in the postoperative setting. Complete CT–DWI correlation tended to be more frequent in preoperative than postoperative examinations, suggesting that postoperative CT may overestimate the true extent of recurrent cholesteatoma because of granulation tissue, fibrosis, middle ear effusion, or other nonspecific inflammatory changes. Although this difference did not reach statistical significance, probably because of the limited sample size, the observed pattern is clinically relevant. Previous pediatric studies have likewise emphasized the value of non-EPI DWI for postoperative surveillance while recommending that MRI findings be interpreted together with conventional imaging, particularly in the early postoperative period[2,3,7,13]. Daoudi et al. reported limited sensitivity of non-EPI DWI in children and demonstrated that MRI accuracy improved with increasing time after surgery3, whereas Yosefof et al. showed that nearly half of residual cholesteatomas were detected only after at least one previous negative MRI examination[13]. Taken together, these findings support combined interpretation of CT and non-EPI DWI in the postoperative evaluation of pediatric cholesteatoma, where CT-visible soft tissue may overestimate the true extent of recurrent disease.

Non-EPI DWI demonstrated a high detection rate in our series, with diffusion restriction identified in nearly all MRI examinations. Most lesions appeared isointense on T1-weighted images and homogeneously hyperintense on T2-weighted images, whereas postoperative lesions more frequently demonstrated heterogeneous signal characteristics. This greater heterogeneity likely reflects varying amounts of postoperative fibrosis, granulation tissue, middle ear effusion, and recurrent keratin debris, which frequently coexist in the postoperative middle ear[1,7,8]. Interestingly, in one case, surgically confirmed cholesteatoma, MRI demonstrated T1 hyperintensity despite showing diffusion restriction. This finding is consistent with the observations of Baudouin et al., who highlighted that atypical conventional MR signal characteristics may be misleading and should not outweigh positive diffusion-weighted imaging findings7. The mean ADC value in our cohort was 879.5 ± 258.1 × 10^{-6} mm^2/s, which falls within the range previously reported for cholesteatoma (759–1370 × 10^{-6} mm^2/s). Although absolute ADC thresholds vary

according to DWI techniques and MRI systems, quantitative ADC measurements provide useful complementary information for differentiating cholesteatoma from non-cholesteatomatous postoperative soft tissue[8,14–16]. Overall, while conventional MR sequences provide valuable anatomical and tissue-characterization information, they remain complementary to non-EPI DWI, which continues to represent the most reliable MRI sequence for the detection of pediatric cholesteatoma[2,3,7,9].

The present study has several limitations. First, its retrospective design and relatively small sample size limit the statistical power and generalizability of the findings. The absence of a disease-negative reference group precluded assessment of conventional diagnostic performance measures. Second, not all patients underwent both CT and MRI examinations because of the retrospective nature of the study and the long study period, which resulted in some heterogeneity in the available imaging data. Finally, although all examinations were performed according to institutional imaging protocols, minor variations in imaging parameters over the long study period were unavoidable because of the retrospective nature of the study. Despite these limitations, the diagnostic integrity of the study remains high, as it relied exclusively on surgically and histopathologically confirmed pediatric cholesteatoma and evaluated both preoperative and postoperative imaging with direct CT–MRI correlation, providing clinically relevant insights into the complementary roles of these imaging modalities.

In conclusion, our findings demonstrate that CT provides valuable anatomical information in pediatric cholesteatoma but has important limitations in the postoperative evaluation of recurrent disease. CT-visible postoperative cavity soft tissue did not always correspond to diffusion restriction, suggesting that CT alone may overestimate the true extent of recurrent cholesteatoma. Non-EPI diffusion-weighted MRI remains the most reliable imaging technique for defining recurrent disease and should be interpreted in conjunction with CT findings when postoperative cholesteatoma is suspected.

Declarations

Ethics Approval: This retrospective study was approved by the Local Ethics Committee (Approval No: İ05-659-26) and the requirement for informed consent was waived because of the retrospective nature of the study.

Conflict of Interest: No conflicts of interest.

Funding: No funding was received for this study.

Data Availability: The datasets generated and/or analyzed during the current study are available from the corresponding author on reasonable request.

REFERENCES

1. Baráth K, Huber AM, Stämpfli P, Varga Z, Kollias S. Neuroradiology of cholesteatomas. AJNR Am J Neuroradiol. 2011;32:221-229. (PMID: 20360335)

2. Lecler A, Lenoir M, Peron J, Denoyelle F, Garabedian EN, Pointe HD, Nevoux J. Magnetic resonance imaging at one year for detection of postoperative residual cholesteatoma in children: Is it too early? Int J Pediatr Otorhinolaryngol. 2015;79:1268-1274. (PMID: 26071017)

3. Daoudi H, Levy R, Baudouin R, Couloigner V, Leboulanger N, Garabédian EN, Belhous K, Boddaert N, Denoyelle F, Simon F. Performance of Non-EPI DW MRI for Pediatric Cholesteatoma Follow-Up. Otolaryngol Head Neck Surg. 2024;170:221-229. (PMID: 37313857)

4. McCallum R, Coleman H, Pervaiz H, Irwin G, McAllister K. Diffusion-weighted magnetic resonance imaging for diagnosis of post-operative paediatric cholesteatoma. J Laryngol Otol. 2023;137:484-489. (PMID: 36184898)

5. Jackson R, Addison AB, Prinsley PR. Cholesteatoma in children and adults: are there really any differences? J Laryngol Otol. 2018;132:575-578. (PMID: 29909808)

6. Molteni G, Fabbris C, Molinari G, Alicandri-Ciufelli M, Presutti L, Paltrinieri D, Marchioni D. Correlation between pre-operative CT findings and intra-operative features in pediatric cholesteatoma: a retrospective study on 26 patients. Eur Arch Otorhinolaryngol. 2019;276:2449-2456. (PMID: 31175451)

7. Baudouin R, Simon F, Levy R, Breton S, Alciato L, Talab E, Leboulanger N, Couloigner V, Garabedian EN, Denoyelle F. Early Magnetic Resonance Imaging to Diagnose Residual Cholesteatoma in Children and Benefit of Radiological Rereview. Otolaryngol Head Neck Surg. 2023;169:1631-1638. (PMID: 37264987)

8. Touska P, Connor SEJ. ESR Essentials: imaging of middle ear cholesteatoma-practice recommendations by the European Society of Head and Neck Radiology. Eur Radiol. 2025;35:2053-2064. (PMID: 39186104)

9. Muzaffar J, Metcalfe C, Colley S, Coulson C. Diffusion-weighted magnetic resonance imaging for residual and recurrent cholesteatoma: a systematic review and meta-analysis. Clin Otolaryngol. 2017;42:536-543. (PMID: 27701821)

10. Molinari G, Reale M, Albera A, Russo FY, Di Lullo AM, Gaffuri M, Ralli M, Turri-Zanoni M, Simon F, Anschuetz L, Trecca EMC. Follow-up strategies in pediatric cholesteatoma: a systematic review. Eur Arch Otorhinolaryngol. 2025;282:11-22. (PMID: 39097857)

11. Finch G, Patel S, Walters B, Trotter M. Factors affecting the correlation between high-resolution computed tomography and operative findings in cholesteatoma surgery - a systematic review. J Laryngol Otol. 2025;29:1-10. (PMID: 40726081)

12. Kul M, Yilmazer Zorlu SN, Özalp Ateş FS, Ünal S. High Resolution Computed Tomography Imaging Findings in Chronic Otitis Media with and Without Cholesteatoma. Kulak Burun Boğaz ve Baş Boyun Cerrahisi Derg. 2023;31:162-9.

13. Yosefof E, Yaniv D, Tzelnick S, Sokolov M, Ulanovski D, Raveh E, Kornreich L, Hilly O. Post-operative MRI detection of residual cholesteatoma in pediatric patients - The yield of serial scans over a long follow-up. Int J Pediatr Otorhinolaryngol. 2022;158:111172. (PMID: 35526314)

14. Lingam RK, Khatri P, Hughes J, Singh A. Apparent diffusion coefficients for detection of postoperative middle ear cholesteatoma on non-echo-planar diffusion-weighted images. Radiology. 2013;269:504-10. (PMID: 23801772)

15. Cavaliere M, Di Lullo AM, Cantone E, Scala G, Elefante A, Russo C, Brunetti L, Motta G, Iengo M. Cholesteatoma vs granulation tissue: a differential diagnosis by DWI-MRI apparent diffusion coefficient. Eur Arch Otorhinolaryngol. 2018;275:2237-2243. (PMID: 30088076)

16. Sheng Y, Hong R, Sha Y, Zhang Z, Zhou K, Fu C. Performance of TGSE BLADE DWI compared with RESOLVE DWI in the diagnosis of cholesteatoma. BMC Med Imaging. 2020;20:40. (PMID: 32306913)